Title

Highly Efficient Exosome Isolation and Protein Analysis by an Integrated Nanomaterial-Based Platform

Journal

Analytical Chemistry, 90(4)

ISSN

0003-2700

Authors

Fang, Xiaoni
Duan, Yaokai
Adkins, Gary Brent
et al.

Publication Date

2018-02-20

DOI

10.1021/acs.analchem.7b04861

Peer reviewed

Published in final edited form as:

Anal Chem. 2018 February 20; 90(4): 2787–2795. doi:10.1021/acs.analchem.7b04861.

Highly Efficient Exosome Isolation and Protein Analysis by Integrated Nanomaterial-based Platform

Xiaoni Fang[1], **Yaokai Duan**[1], **Gary Brent Adkins**[1], **Songqin Pan**[2], **Hua Wang**[1,4], **Yang Liu**[3], and **Wenwan Zhong**[1,3,*]

[1]Department of Chemistry, University of California-Riverside, Riverside, CA 92521, U.S.A

[2]Institute for Integrative Genome Biology, University of California-Riverside, Riverside, CA 92521, U.S.A

[3]Environmental Toxicology Program, University of California-Riverside, Riverside, CA 92521, U.S.A

[4]Yancheng Normal University, Jiangsu, China

Abstract

Exosomes play important roles in mediating intercellular communication and regulating a variety of biological processes, but clear understanding of their functions and biogenesis has not been achieved, due to the high technical difficulties involved in analysis of small vesicular structures that contain a high proportion of membrane structures. Herein, we designed a novel approach to integrate two nanomaterials carrying varied surface properties, the hydrophilic, macroporous graphene foam (GF) and the amphiphilic periodic mesoporous organosilica (PMO) for efficient exosome isolation from human serum and effective protein profiling. The high specific surface area of GF, after modification with the antibody against the exosomal protein marker, CD63, allowed highly specific isolation of exosomes from complex biological samples with high recovery. Since the organic solvent, methanol, turned out to be the most effective lysis solution for releasing the exosomal proteins, the amphiphilic PMO was employed to rapidly recover the exosomal proteins, including the highly hydrophobic membrane proteins. The fine pores of PMO also acted as the nano-reactors to accelerate protein digestion that produced peptides subject to LC-MS/MS analysis. A total of 334 proteins with 111 membrane proteins (31% of these contained > 2 transmembrane domains (TMD)) were identified using the integrated GF/PMO platform. In contrast, with the commercial exosome isolation kit and the in-solution protein digestion method, only 151 proteins were found with 28 being membrane proteins (only 1 contained 3 TMDs). Our results support that the integrated GF/PMO platform is of great value to facilitate the

*Corresponding Authors: wenwan.zhong@ucr.edu, Fax: +1 951 827 4713.
ORCID
Wenwan Zhong: 0000-0002-3317-3464

Notes

The authors declare no competing financial interest. Serum samples were obtained with informed consent.

Supporting Information

Characterization of materials, NTA counting of exosomes change before and after isolated by GF@PD-CD63 and GF@PD-CD63&PEG, BCA quantify the lysed exosomes under different conditions, Venn diagrams of the proteins identified with our method, 60% methanol and FASP, and exosomal membrane protein identified by the integrated nanomaterial-based platform were listed in supplementary information. This material is available free of charge via the Internet at http://pubs.acs.org.

comprehensive characterization of exosomal proteins for better understanding of their functions and for identification of more exosome-based disease markers.

Graphical Abstract

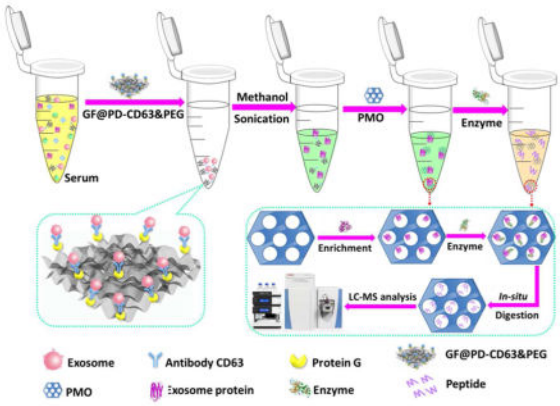

Introduction

Extracellular vesicles (EVs) are membranous structures released into extracellular space by cells, and carrying cargos like proteins and nucleic acids.[1–4] There are multiple types of EVs, including exosomes, microvesicles (MV), and apoptotic bodies, and they differ in size, cellular origin, secretion pathways, and functionality.[5–7] Among them, exosomes are the most frequently studied because of their important roles in mediating intercellular communication and regulating a variety of biological processes, such as immune response, tumor-igenesis and metastasis.[8–10] Exosomes are small EVs with diameters around 30–150 nm and secreted by most eukaryotic cells.[11–14] Release of exosome has been found to increase significantly in most neoplastic cells and occur continuously at all stages of tumor development.[15,16] Therefore, accumulation of the tumor-derived exosomes in blood and malignant effusions has been widely reported.[17–20] Growing evidences have shown that the tumor-derived exosomes carry characteristic proteins and RNAs in various cancer types and the expression levels of these molecules are closely correlated with tumor progression.[21–23] These exosomal markers may constitute a “cancer signature” to facilitate early detection and progression monitoring of tumors in a non-invasive manner.[24,25] In addition, exosomes and their contents could be the targets for new, effective therapeutics if their functions in regulating tumor origination and progression could be revealed. However, efficient isolation, molecular classification, and comprehensive characterization of these extremely small and molecularly diverse vesicles are very challenging. The current state-of-the-art techniques for exosome isolation are far from maturity to overcome the technical challenges, severely impeding extensive biological and clinical studies of exosomes.

Numerous exosome isolation techniques have been established by far, including ultracentrifugation, polymer-based precipitation, filtration, and affinity pull-down. Currently the most common method for exosome purification is ultrafiltration, which includes several centrifugation steps reaching speeds of up to 200,000 × g.[26,27] Nevertheless, it always turns

out to have low recovery (~ 5–25%) and involves tedious procedures.[27] Polymer-based precipitation rely on the formation of polymer network to entangle all lipid components in the sample and reduce their solubility for rapid removal under a low centrifugal force.[28,29] Although quick and simple, such methods always suffer from the inclusion of non-exosomal contaminants, and the polymers used, like polyethylene glycol (PEG), are incompatible with the down-stream analysis. Membrane filtration has also been applied for size-based isolation of exosomes, but exosomes are prone to adhere to the filtration membranes and become lost for the following analysis.[30–32] Moreover, the additional force applied to pass the analyzed liquid through the membranes could potentially deform or damage the exosomes.

While these physical isolation methods can handle large sample volumes and deliver exosomes with sufficient quantities for down-stream analysis, it is difficult for them to obtain exosomes of high purity, because of the presence of other membrane-derived subcellular structures with high similarity in physical properties to exosomes, such as apoptotic vesicles, membrane particles, and ectosomes.[33–36] Affinity pull-down is superior in selective separation of exosomes using specific antibodies. However, the high purity is offset by the lack of quantity, preventing thorough genomic and proteomic analysis of the exosomal contents if sample supply is limited. In particular, exosomes have large surface areas but small absolute volumes, and thus a large proportion of exosomal proteins are membrane proteins, which present great challenges in proteomic analysis. Thus, techniques that can smoothly integrate efficient exosome isolation with downstream molecular profiling are in great demand.

Herein, we report a new method that integrates affinity pull-down and membrane protein enrichment for efficient exosomal protein profiling (Figure 1). Our method takes advantage two sets of nanomaterials (NMs) that have unique but opposite properties, one being hydrophilic and macro-porous, and the other being amphiphilic and mesoporous. The macro-porous graphene foam (GF) holds extremely large specific surface areas, contains pores fit well by the exosomes, and possesses abundant hydrophilic groups for antibody attachment. These features are highly favorable for the design of an affinity pull-down platform for exosomes. On the other hand, the isolated exosomes are lysed; and the resultant proteins are enriched by the amphiphilic periodic mesoporous organosilica (PMO) that, besides an extractor for proteins, provide pores to be the nano-reactors for *in situ* proteolytic digestion of the exosomal proteins. As a result, the integrated GF-PMO platform can specifically isolate exosomes, enrich the highly hydrophobic exosomal proteins, and process the proteins in situ with minimum sample loss. To prove the effectiveness of this platform, it was applied to isolate exosomes present in serum and analyze their protein contents. A total of 334 proteins with 111 membrane proteins were identified compared to only 28 membrane proteins found from the same sample using a commercial kit for exosome isolation and direct protein digestion without PMO-assisted processing.

Experimental Section

Chemicals and Bioreagents

Graphene oxide (GO), poly(ethylene oxide)-poly(propylene oxide)-poly(ethylene oxide) (PEO-PPO-PEO) triblock copolymers ($EO_{106}PO_{70}EO_{106}$, Pluronic F127),

bis(trimethoxysilyl)ethane (BTME), 1,3,5-trimethylbenzene (TMB), dithothreitol (DTT), iodoacetamide (IAA), sodium deoxycholate, sodium lauroyl sarcosinate, protease inhibitor cocktail, potassium chloride, and the wild-type bacteriorhodopsin (BR) isolated from Halobacterium salinarum strain S9 were obtained from Sigma-Aldrich (St. Louis, MO). Recombinant Protein G (Protein G), Invitrogen Total Exosome Isolation kit and the amine-modified polyethylene glycol (NH_2-PEG) were ordered from Thermo Scientific. The recombinant protein of CD 63 (bioti-nylated, human) was purchased from Biolegend. Purified exosomes were purchased from Galen Laboratory Supplies (North Haven, CT). All reagents were used directly without further purification. Deionized water (18.4 MR) used for all experiments was obtained from a Milli-Q system (Millipore, Bedford, MA).

Synthesis and characterization of GF and PMO materials

Graphene foam (GF) was prepared using the method reported by Chen et al.[37] In brief, phytic acid was employed as the gelator and dopant, and graphene oxide (GO) acted as the precursor. Briefly, GO was suspended in 15 mL water to reach a concentration of 2 mg/mL, and applied with 0.5 mL PA. The mixture was sonicated for 40 min at room temperature, and then the mixture was sealed in a 25 mL Teflon-lined autoclave tube and reacted at 180 °C for 12 hrs. After cooling down the autoclave tube to room temperature, the solid precipitate formed from the reaction was collected by tweezer and washed by ethanol and water thoroughly. At last, the GF product was freeze-dried and stored as a solid until usage.

PMO was synthesized according to the previously reported method as well.[38] At first, 0.5 g of F127, 2.5 g of KCl, and 0.5 g of TMB were dissolved in 30 g of HCl (0.1 M), and supplied with 2.0 g of BTME after the mixture was stirred for 6 hrs at 0 °C. And then, the solution was stirred for 24 h at room temperature, the resultant mixture was hydrothermally treated at 100 °C for another 24 hrs. Subsequently, the resultant powder was filtered and washed by ethanol and 2 M HCl at 60 °C to remove the residual template. The final PMO products were obtained by filtration and dried at room temperature in air.

Transmission electron microscopy (TEM) image was directly taken with a JEOL 2011 microscope operated at 200 kV with the samples dispersed on a Cu grid coated by carbon films. Scanning electron microscope (SEM) image was obtained by SUPERSCAN SSX-550 scanning electron microscope (Shimadzu, Japan). The exosomes were viewed by SEM after being coated with gold and fixed by glutaraldehyde and ethanol, respectively. The infrared spectra were obtained by the FTIR 360 manufactured by Nicolet (Thermofisher, USA). X-ray photoelectron spectrometer (PerkinElmer PHI 5000C ESCA System) equipped with Mg Ka radiation was used to the collection of X-ray photoelectron spectroscopy (XPS) data.

Immobilization of anti-CD63 on GF for affinity pull-down of exosomes

The poly-dopamine-functionalized graphene foam (GF@PD) was synthesized by an *in-situ* polymerization method. Briefly, dopamine hydrochloride was dissolved in 10 mL of Tris (10 mM, pH 8.5), and GF were added to the concentration of 1 mg/mL. The mixture was stirred for 24 hrs at room temperature, and then the solution was centrifuged to precipitate the GF@PD, which was washed by deionized water thoroughly. Next, 1 mg of GF@PD and 20 μg/mL of protein G were mixed in 1×PBS, and incubated for 16 hrs at room temperature.

The protein G in excess was washed away by 1×PBS, before 20 μg/mL of the anti-CD63 IgG was added. To prevent non-specific adsorption of the interfering components in biological samples, NH_2-PEG was mixed with GF@PD-CD63 to form the composites of GF@PD-CD63&PEG. The primary amine on PEG mediated adsorption via H-bonding with the rich –OH group of PD.

Isolation of exosomes by GF@PD-CD63&PEG

Briefly, 10 μg of GF@PD-CD63&PEG was added into 10 μL of the purchased exosomes at 0.1 Zg/ZL in 1× PBS, and the mixture was stirred gently on ice for 30 min. The suspension was centrifuged at 10,000×g for 10 min and the supernatant was collected for fluorescence measurement and NTA counting to quantify the remained exosomes. A similar protocol was used to study exosome isolation from serum. If protein analysis was to be carried out after removing the supernatant, the precipitated exosome was re-suspended in methanol and lysed.

Enrichment and processing of exosomal proteins assisted by PMO

Exosomes suspended in methanol was sonicated on ice for 1 hr, and centrifuged at 8,000×g for 5 min to remove the GF@PD-CD63&PEG. The supernatant was collected, which contained the exosomal proteins, and freeze-dried. Then the proteins were re-dissolved in the Ammonium-Bicarbonate buffer (ABC buffer, 25 mM, pH 8.0, 10 μL); reduced by 50 mM DTT at 37 °C for 2 hrs and then alkylated with 55 mM IAA for another 1 hr at room temperature in dark. Then, 10 ZL methanol was added and sonicated on ice for 15 min to ensure through solubilisation of the membrane proteins. Followed, the amphiphilic PMO was added to the protein solution and incubated at room temperature for 30 min to extract the proteins from the organic phase. Once the PMO was pelleted by centrifugation at 10,000×g and resuspended in 15 μL of the ABC buffer, 5 μL of trypsin was dissolved in the same buffer with an enzyme/substrate ratio of 1:10 (w/w) and the mixture was incubated at 37 °C for 2 hrs. Subsequent to the proteolytic digestion, the mixture was centrifuged; and the precipitate was resuspended in 0.1% TFA/50% ACN aqueous solution (v/v) and shaken for 30 min to elute the digested peptides from the PMO, which was then subsequently removed by centrifugation. Finally, the eluted peptides were collected and purified by Zip-Tip, ready for LC-MS/MS analysis.

For comparison, exosomes isolated by the Invitrogen Total Exosome Isolation kit from the same serum sample were digested in solution according to the reported method.[39] Briefly, the isolated exosomes was dissolved in 50 μL methanol and sonicated on ice for 1 hr. The proteins were freeze-dried and re-dissolved in 10 μL ABC buffer. After the proteins were reduced with DTT and alkylated with IAA, 5 μL of trypsin was added into the mixture and incubated at 37 °C for 2 hrs. The subsequent treatment of the resultant peptides were the same as described above.

LC-MS/MS conditions

The peptides obtained from exosomes were subjected to chromatographic separation with a nano Acquity UPLC system (Waters Corporation, Milford, MA) that was connected to a LTQ orbitrap mass spectrometer (Thermo Fisher Scientific, San Jose, CA) equipped with an

online nano-ESI ion source (Michrom Bioresources, Auburn, CA). Sample was dissolved in 0.2% formic acid in water and then injected into a reverse phase column (BEH C18, 75 Zm x 20 cm, Waters Corporation, Milford, MA) at a flow rate of 0.3 μL/min. The column temperature was maintained at room temperature. The mobile phase consisted of solvent A -- 0.2% formic acid in water; and solvent B -- 0.2% formic acid in acetonitrile. The LC run started with 3% B and continued for 2 min, followed by a gradient increase to 35% B in 50 min, and then increased to 85% B in 5 min. At the end of the run, the column was allowed to equilibrate at 3% B for 5 min. The mass spectrometer was working under a data-dependent mode. For every duty cycle, one full-MS survey scanned within a mass range of 300–1800 Da with a resolving power of 100,000 was obtained, and then the scan was switched automatically to the MS/MS mode for the 10 strongest peaks in the LTQ section. Higher energy CID (HCD) was used for fragmentation activation with 30% normalized activation.

Database Search and Data Analysis

The raw MS files were analyzed by MaxQuant, version 1.4.1.2. MS/MS spectra were searched by the Andromeda search engine against the decoy SwissProt-human database (Release 2014-04-10) containing the forward and reverse sequences (total of 40,492 entries). In the main Andromeda search, the precursor mass and fragment mass had an initial mass tolerance of 5 ppm and 20 ppm, respectively. The search included variable modifications of methionine oxidation and N-terminal acetylation, and fixed modification of carbamidomethyl cysteine. The minimal peptide length was set to seven amino acids, and the search allowed a maximum of two miscleavage sites. The false discovery rate (FDR) was set to 0.01 for peptide and protein identification.

The grand average of hydrophobicity (GRAVY) values of the identified exosomes membrane proteins were obtained using ProtParam (http://tw.expasy.org/tools/protparam.html). The proteins with positive and negative GRAVY values were named as hydrophobic and hydrophilic proteins, respectively. The TMD of the identified proteins were predicted by using the transmembrane hidden Markov model (TMHMM, http://www.cbs.dtu.dk/services/TMHMM/) algorithm. Proteins with more than one predicted TMD were categorized as membrane proteins in our work.

Results and Discussion

Characterization of the GF and PMO

The GF and PMO used in this study were characterized by various techniques. The SEM image of GF (Figure 2a) showed its highly porous (pore size ~ 10 Zm in diameter) and foam-like structure constructed from the graphene sheets. Further characterization by TEM illustrated the wrinkled and folded layers of GF (Supporting Information, Figure S1a). The foam-like structures provide high specific surface area to enhance protein immobilization and exosome binding. Elemental analysis by XPS confirmed the presence of the hydrophilic oxygen-containing groups, such as the hydroxyl/epoxyl groups, on GF surface, as well as the successful integration of PA that supplied the abundant phosphate groups (Supporting Information, Figure S1b). The chemical bonds of P=O, P-O-C (phosphate ester group), P-O, and P-O-H, were clearly detected by Fourier transform infrared (FT-IR) spectroscopy

(Supporting Information, Figure S1c). The phosphate groups permitted strong adsorption of dopamine via electrostatic attraction, which underwent *in-situ* oxidative polymerization and formed a cover of poly-dopamine (PD) on GF surface. Comparison of the FT-IR spectra of GO, GF, and the PD-modified GF (Figure 2b) revealed the presence of the absorption peaks at 3343 and 1147 cm^{-1} on GF@PD, which can be assigned to the O-H and C-N stretching vibration, respectively. In addition, new bands at 1261 cm^{-1}, 1060 cm^{-1} and 870 cm^{-1} corresponded to the C-O, C-O-H and Ar-H bending vibration of PD. These results prove that GF was fabricated and successfully modified with PD.

The PMO prepared in this work contained relatively uniform pores with the diameter around 20 nm and the p6mm structure symmetry as seen by SEM (Figure 2c). The FT-IR spectrum of PMO (Figure 2d) contained the multiple peaks at 1,000~1100 cm^{-1}, which were from the Si-O bond and the Si-OH groups. The peak at 2920 cm^{-1} can be assigned to the -CH_2- groups. All these features of PMO can help with enrichment and digestion of the exosomal proteins. The meso-pores can serve as the nanoreactors to speed up the tryptic digestion of the adsorbed exosomal proteins. The reaction time can be significantly reduced owing to the tight confinement of the proteins and enzymes in a narrow pore space. The presence of both the -CH_2- and the Si-O-Si groups makes the surface of PMO amphiphilic, compatible with both water and organic solvents. Therefore, methanol can be first used to lyse exosome and well solubilize the resultant proteins, a significant proportion of which are membrane proteins. The enriched proteins can then be co-precipitated with PMO and redissolved in the aqueous ABC buffer to accommodate trypsin digestion.

Antibody immobilization and affinity pull-down of exosomes

Affinity-based isolation provides higher specificity than the physical isolation methods, and thus is better suited for exosome isolation from complex biological matrices. Surface immobilization of antibody is usually carried out through binding to bridging molecules such as protein G or protein A to preserve the appropriate orientation of IgG and high affinity and specificity to the targets. To immobilize protein G on the GF surface, we employed the simple modifier, dopamine. Dopamine (DA) has been identified by Lee *et al.*[40,41] as a revolutionary tool in surface functionalization, because under basic conditions, DA rapidly polymerizes and the resultant poly-dopamine coating makes the surface highly adhesive to proteins and cells.[42–44] Thus, protein G can be adsorbed on the surface of GF@PD, which can then be used to immobilize the antibody against exosomes. We targeted CD63, the general marker of exosomes representative to its endosomal origin, in the present work, and thus anit-CD63 was employed. The quantities of protein G and anti-CD63 immobilized on GF@PD were evaluated using the Bradford assay (BCA). As shown in Figure 3a, more than 70% of the protein G in solution was adsorbed by GF@PD, loading 15.49±6.6 μg protein G per mg of GF@PD. The successful functionalization of protein G ensured the high conjugation efficiency in the subsequent antibody immobilization: anti-CD63 was adsorbed onto the protein G modified GF@PD surface at a comparable loading 14.88±1.9 μg anti-CD63 per mg GF@PD to that of protein G.

If the adsorbed protein G and anti-CD63 do not fully cover the highly adhesive polydopamine surface, non-specific adsorption would occur when the material is applied in

complex biological samples. To eliminate non-specific adsorption, we further coated GF@PD with PEG after anti-CD63 immobilization (GF@PD-CD63), and tested protein adsorption in human serum. The total protein concentration in serum was quantified by the Braford assay before and after treatment with the anti-CD63 modified GF@PD, and comparison was made between the materials with and without the PEG coating (Figure 3b). We can see that, both materials reduced the protein concentration in serum, and the amounts of proteins washed off by 1×PBS from both materials were comparable: about 29.3 mg/mL proteins were eluted off from the non-PEG coated GF@PD, while 21.2 mg/mL was found from the PEG-coated material, with no significant difference when subject to t-test. This result indicates that, protein G and anti-CD63 already provided sufficient surface coverage to deactivate the adsorption sites on the polydopamine modified surface, and the remaining, weak non-specific adsorption can be removed by washing with solutions containing high salt contents. The proteins removed by GF@PD-CD63 should be included in the CD63-containing, which were released upon treatment with the lysis solution (100% methanol), and quantified by BCA. Both the GF@PD-CD63 with or without PEG coating yielded a comparable amount of proteins (Figure 3b, column D and H).

To fully evaluate the effect of exosome isolation by the antibody and PEG modified GF@PD, a more systematic investigation was carried out using NTA and fluorescence spectroscopy. The purified exosomes were employed and stained with the lipophilic dye of DiO. This dye becomes highly fluorescent when bound to lipid structures and can be used to illustrate the presence of lipid vesicles. We observed a large reduction in fluorescence after the stained vesicles were incubated with both GF@PD-CD63 with or without PEG coating, and both led to comparable fluorescence in the supernatant after exosome isolation (Figure 3c), indicating that PEG coating on GF@PD-anti-CD63 did not prevent exosome binding. In addition, the particle concentration of the exosome solution was found to be more than 1×10^8 particles/mL by NTA before isolation, and decreased to 5.6×10^6 particles/mL after isolation by the prepared materials (Figure S2, Supporting Information). We also compared the isolation efficiency between the Invi-trogen Total Isolation kit and the GF@PD-CD63&PEG method. As shown in Figure S3 (Supporting Information), the fluorescence of DiO dropped after the standard exosomes were either precipitated by the Invitrogen kit or by our GF@PD-CD63 method; but the GF@PD-CD63&PEG yielded a lower fluorescence, supporting that it removed more exosomes than the Invitrogen kit. Exosomes captured by GF@PD-CD63&PEG were imaged by SEM (Figure 3d). Compared with the bare GF (Figure 2a), GF@PD and GF@PD-CD63 (Figure S4, Supporting Information), a high density of exo-somes particles were found on the surface of GF@PD-CD63. These results support that anti-CD63 modification on GF@PD led to successful exosome binding, and PEG coating which could eliminate the non-specific adsorption of protein exhibited no obvious influence on exosome isolation efficiency.

Exosome lysis and protein recovery

Exosomal protein profiling can help to study exosome function and content packaging, but requires effective methods to lyse the vesicles and recover the proteins, in addition to successful exosome isolation demonstrated above. We compared the vesicle breakup effects from several well-adopted lysis solutions, including pure methanol, the hypertonic ABC

buffer (25 mM ammonium bicarbonate), and the surfactant-containing buffers - RIPA (0.5 M Tris-HCl, pH 7.4, 1.5 M NaCl, 2.5% deoxycholic acid, 10% NP-40, 10 mM EDTA), and SST (12 mM sodium deoxycholate, 12 mM sodium lauroyl sarcosinate). Except for methanol, the lysis solutions were supplied with the protease inhibitor cocktail in 100 mM Tris]HCl to prevent protein degradation before trypsin digestion.

Ten μL of the exosome standard was mixed with 200 ZL of the lysis solution. Effective lysing should damage the vesicle structure and release free proteins, thus the particle number in the solution should decrease, along with increase in protein concentrations detected in the supernatant. Therefore, we monitored the particle number by NTA in the mixture at various reaction duration, and also measured the total protein concentration in the solution by BCA after the reaction proceeded for 60 min. The effect of sonication was evaluated as well. The results (Figure S5, Supporting Information) show that the largest reduction in particle concentration was achieved with methanol, followed by the RIPA or SST buffer (Fig. S5a). Lysis duration of 60 min was sufficient to reach maximum particle reduction. Sonication during lysis further reduced the number of particles. Correspondingly, methanol yielded more proteins than others; and sonication added about 20% (for other buffers) - 30% (for methanol) more proteins to the supernatant (Fig. S5b). The excellent performance of methanol could be attributed to the high solubility of the hydrophobic lipids and membrane proteins in organic solvents.

Methanol was then applied to release the proteins from the exosomes isolated with GF@PD-CD63&PEG. One mL of the exosome-containing sample -- either the standard suspension in 1×PBS at 0.1 Zg/ZL (total protein concentration in exosomes) or human serum -- was incubated with 1 mg of GF@PD-CD63&PEG for 30 min. The GF was then precipitated from the supernatant by centrifugation, washed thoroughly with 1×PBS, mixed with methanol and sonicated for 60 min. The proteins extracted by the GF@PD-CD63&PEG were dried and subject to SDS-PAGE. The supernatant was also dried and treated with methanol before analyzed on gel. The amount of CD63 was quantified by Western Blot. Exosomes recovered by GF@PD-CD63&PEG from the exosome standard solution and from serum (Lane #4 and #7, respectively, in Fig. 4a) exhibited similar amounts of CD63 as in the solutions before extraction (Lane #2 and #5, respectively, in Fig. 4a). But the amounts of CD63 remained in the supernatant from both solutions after affinity pull-down (Lane #3 and #6) were not detectible. Using the calibration curve established with the pure CD63 protein (Lane #8-10), we calculated the amounts of the exosomal CD63 in Lane #2, 4, 5, & 7, and plotted them in Figure 4b. More than 70% of the serum CD63 was isolated by GF@PD-CD63&PEG. Exosome extraction from the standard solution yielded a recovery ~150%, which may be the result of elution of the adsorbed anti-CD63 off GF by methanol when fewer proteins were isolated from the standard solution. This antibody is the same as the primary antibody used in Western Blot. Due to the diffusion of the CD63 band (commonly seen in works reporting WB results for CD63), which overlapped with that of the light chain of IgG, the eluted anti-CD63 might be included in the CD63 band and detected by the secondary antibody. Nevertheless, the above results confirmed again the high exosomes recovery obtained with the modified GF owing to its high specific surface area.

Improved exosomal protein identification by the integrated nanomaterial-based platform

The results shown above indicate that we can isolate exosomes with high recovery by GF@PD-CD63&PEG and lyse them effectively by methanol coupled with sonication. However, a large proportion of the exosomal proteins are membrane proteins because of its high surface-area-to-volume ratio, protein identification could be hindered if the membrane proteins are not treated appropriately.[45,46]

Numerous membrane proteins enrichment, solubilization, digestion, and fractionation techniques have been developed to assist the identification of membrane proteins, including a mini-ball mill method for solvent-free matrix assisted laser desorption ionization mass spectrometry (MALDI-MS), two-phase or on-membrane digestion approach, centrifugal proteomic reactor, etc.[47–51] However, these existing methods are time-consuming, high-cost, and labor intensive. Recently, filters-aided sample preparation (FASP) developed by the Mann group has been widely employed in membrane protein analysis, providing various advantages like fast reaction kinetics, high digestion efficiency, and low operation cost.[52,53] Nevertheless, sodium dodecyl sulfate (SDS) was involved in FASP method which can inhibit protease activity, decrease separation efficiency, and interfere with the subsequent MS detection. Additionally, removal or dilution of the detergent additives is indispensable and needs to be done by multiple washing steps before tryptic digestion and MS analysis in these protocols, which would lead to poor recovery of the membrane proteins and prevent sensitive detection of proteins. Our approach is to take advantage of the amphiphilic PMO, which can serve not only as an extractor for the hydrophobic membrane proteins, but also a nanoreactor for efficient protein digestion.[54] While methanol can enhance the solubility of membrane proteins, methanol cannot be the solvent for protein digestion.[55] PMO can be dissolved well in methanol and provide large and compatible binding surface to enrich the proteins. Upon enrichment, PMO can then be precipitated easily to realize convenient buffer exchange. Once the PMO with the enriched proteins is exchanged to the protease-compatible buffer, protein digestion can be carried out effectively.

We initially found that PMO could enrich diverse proteins including membrane proteins with recovery higher than 85% (Figure S6, Supporting Information). We then further tested the effect of coupling PMO with the GF-based immuno-isolation in enhancing identification of exosomal proteins. One mg of GF@PD-CD63&PEG was mixed with 1 mL serum to pull down the exosomes, which was precipitated by centrifugation and subsequently treated with 1 mL methanol coupled with sonication to release the exosomal proteins. Upon removal of the GF@PD-CD63&PEG, The protein solution was freeze-dried, and treated with 10 ZL ABC buffer supplied with IAA and DTT to denature the proteins. Then 10 ZL of methanol was added and sonicated for 15 min, before the PMO was added at a final concentration of 1 mg/mL to extract the proteins. The PMO was precipitated by centrifugation and re-suspended in 20 μL of the ABC buffer for tryptic digestion. We compared the digestion duration of 2 and 12 hours, and found no difference in the total number and types of proteins identified (Figure S7, Supporting Information). The rapidness in protease digestion on PMO surface can be attributed to its amphiphilic property that is not only suitable for enrichment of membrane proteins from organic phase (methanol), but also good for dispersion in aqueous solutions to maintain high pro-tease activity. The mesoporous 3D nanostructure can

also accelerate *in situ* proteolysis because the nanopores provide high relative surface areas, and co-localize both the proteins and the enzyme within the pores for faster reaction. Therefore, we chose the shorter digestion time of 2 hrs in the present work. For comparison, exosomes from the same volume of serum were isolated by the Invitrogen Total Exosome Isolation kit and directly digested in the ABC solution, which represented the conventional method. The results were displayed in Figure 5.

A total of 1,387 peptides and 334 proteins were identified with the integrated platform of GF@PD-CD63&PEG/PMO (referred to GF/PMO in later text) in three independent repeats with good batch-to-batch reproducibility (Figure S8, Supporting Information);, while only 151 proteins found with the traditional approach, only 54 from which were missed by the integrated nanomaterial-based platform (Fig. 5a). Plotting the molecular weight and isoelectric point (PI) of these proteins (Fig. 5b), we can see proteins with a wide range of properties were identified: the molecular weight of the identified proteins was between 5.98 and 552.04 Da and their isoelectric points ranged from 4.42 to 11.19.

To evaluate the effectiveness of our integrated platform in improvement of exosomal protein analysis, we obtained the gene oncology (GO) information for the proteins found in both methods by searching the PANTHER database.[56–57] To facilitate analysis and visualization, only a selected subset of the GO terms, i.e. the “PANTHER GO-slim“ was used to obtain information about the molecular functions the protein plays and the cellular components where it functions. Among the identified proteins, 275 from the integrated platform and 118 from the conventional method were annotated and included in this search (Figure S9, Supporting Information). The GF/PMO platform gave out about 2-fold enhancement in the percentage of membrane proteins compared to that found with the conventional method (10.4% vs. 4.9%); and it found more proteins carrying the receptor (10.1% vs. 4.7%) and transporter (13.8% vs. 3.1%) activities.

Further analysis using the transmembrane hidden Markov model (TMHMM) revealed that 111 of the 334 identified proteins are integral membrane proteins, including the distinct exosomal markers like CD63 and CD81, whereas the traditional method just found 28 membrane proteins. The detailed information on the identified exosomes membrane proteins is listed in Table S1 (Supporting Information). TMHMM analysis can reveal the number of transmembrane domains (TMDs) of the identified membrane proteins. As illustrated in Figure 6a, more membrane proteins with higher than 2 TMDs (a total of 35 proteins, ~31% of the total membrane proteins found) identified by our method, compared to only 1 of such proteins was discovered by the conventional method. The GRAVY values of the membrane proteins were also analyzed (Figure 6b). Our method identified 9 times more hydrophobic proteins (GRAVY ≥ 0) and 3.4 times more of the hydrophilic proteins (GRAVY ≤ 0) than the traditional method. These results demonstrate the great potential of the integrated GF/PMO platform towards exosomal protein analysis.

We also compared the effectiveness in membrane protein analysis using our platform with the two widely used methods that either employs 60% methanol to facilitate membrane dissolution, or a filter device to assist with membrane protein handling, i.e. FASP. These two methods were applied on the exosomes isolated with the Invitrogen Total Exosome Isolation

kit (Supporting Method in Supporting Information). The results were displayed in Figure S10 (Supporting Information). A total of 223 proteins were identified using 60% methanol, and the FASP method identified only 181 proteins, both numbers smaller than that identified with our platform. Moreover, TMHMM analysis found only 55 membrane proteins (including CD63) with 60% methanol and 67 (including both CD63 and CD 81) with FASP, while >100 membrane proteins were found with our platform. Deep membrane proteomics analysis further confirm that our method can identify membrane proteins with longer TMD and higher hydrophobicity than these two modified methods.

Conclusions

In summary, we present a novel, integrated platform coupling the macroporous and hydrophilic GF with the mesoporous and amphiphilic PMO for efficient exosomes capture from complex biological samples and effective exosomal protein profiling. More membrane proteins can be identified compared to conventional methods. Such a platform is a valuable tool for study of exosome functions and will have broad applications in protein profiling of diverse intra- or extra-cellular vesicles.

Supplementary Material

Refer to Web version on PubMed Central for supplementary material.

Acknowledgments

The authors would like to thank the support by the National Cancer Institute of the National Institutes of Health under Award Number R01CA188991 to W. Zhong; and the Research Training Grant in Environmental Toxicology from the National Institute of Environmental Health Sciences (T32ES018827) to G. B. Adkins.

References

1. Kalra H, Drummen GPC, Mathivanan S. Int J Mol Sci. 2016; 17:170. [PubMed: 26861301]
2. Turturici G, Tinnirello R, Sconzo G, Geraci F. Am J Physiol Cell Physiol. 2014; 306:C621. [PubMed: 24452373]
3. Pegtel DM, Peferoen L, Amor S. Philos T R Soc B. 2014; 369
4. Dakubo, GD. Cancer Biomarkers in Body Fluids: Principles. In: Dakubo, GD., editor. Spr Int Pub: Cham. 2016. p. 233-260.
5. Raposo G, Stoorvogel W. J Cell Biol. 2013; 200:373. [PubMed: 23420871]
6. Minciacchi VR, Freeman MR, Di Vizio D. Semin Cell Dev Boil. 2015; 40:41–51.
7. Wan Y, Cheng G, Liu X, Hao S-J, Nisic M, Zhu C-D, Xia Y-Q, Li W-Q, Wang Z-G, Zhang W-L, Rice SJ, Sebastian A, Albert I, Belani CP, Zheng S-Y. Nature biomedical engineering. 2017; 1:0058.
8. Zhao L, Liu W, Xiao J, Cao B. Cancer Lett. 2015; 356:339–346. [PubMed: 25449429]
9. Chen X, Liang H, Zhang J, Zen K, Zhang CY. Trends Cell Biol. 2012; 22:125–132. [PubMed: 22260888]
10. Muralidharan-Chari V, Clancy JW, Sedgwick A, Souza-Schorey C. J Cell Sci. 2010; 123:1603. [PubMed: 20445011]
11. Thery C, Zitvogel L, Amigorena S. Nat rev Immunol. 2002; 2:569–579. [PubMed: 12154376]
12. Ha D, Yang N, Nadithe V. Acta Pharm Sin B. 2016; 6:287–296. [PubMed: 27471669]
13. Lai CP, Mardini O, Ericsson M, Prabhakar S, Maguire CA, Chen JW, Tannous BA, Breakefield XO. ACS Nano. 2014; 8:483–494. [PubMed: 24383518]
14. Aryani A, Denecke B. Mol Neurobiol. 2016; 53:818–834. [PubMed: 25502465]

15. Azmi AS, Bao B, Sarkar FH. Cancer Metast Rev. 2013; 32doi: 10.1007/s10555-10013-19441-10559
16. Nuzhat Z, Kinhal V, Sharma S, Rice GE, Joshi V, Salomon C. Oncotarget. 2017; 8:17279–17291. [PubMed: 27999198]
17. Ashby J, Flack K, Jimenez LA, Duan Y, Khatib AK, Somlo G, Wang SE, Cui X, Zhong W. Anal Chem. 2014; 86:9343–9349. [PubMed: 25191694]
18. Doldán X, Fagúndez P, Cayota A, Laíz J, Tosar JP. Anal Chem. 2016; 88:10466–10473. [PubMed: 27734678]
19. Wang S, Zhang L, Wan S, Cansiz S, Cui C, Liu Y, Cai R, Hong C, Teng IT, Shi M, Wu Y, Dong Y, Tan W. ACS Nano. 2017; 11:3943–3949. [PubMed: 28287705]
20. Wan S, Zhang L, Wang S, Liu Y, Wu C, Cui C, Sun H, Shi M, Jiang Y, Li L, Qiu L, Tan W. J Am Chem Soc. 2017; 139:5289–5292. [PubMed: 28332837]
21. Shao H, Chung J, Lee K, Balaj L, Min C, Carter BS, Hochberg FH, Breakefield XO, Lee H, Weissleder R. Nat Commun. 2015; 6:6999. [PubMed: 25959588]
22. Henderson MC, Azorsa DO. Frontiers in Oncology. 2012; 2:38. [PubMed: 22649786]
23. Zhang X, Yuan X, Shi H, Wu L, Qian H, Xu W. J Hematol Oncol. 2015; 8:83. [PubMed: 26156517]
24. Crowley E, Di Nicolantonio F, Loupakis F, Bardelli A. Nat Rev Clin Oncol. 2013; 10:472. [PubMed: 23836314]
25. Zou G, Benktander JD, Gizaw ST, Gaunitz S, Novotny MV. Anal Chem. 2017; 89:5364–5372. [PubMed: 28402650]
26. Liga A, Vliegenthart ADB, Oosthuyzen W, Dear JW, Kersaudy-Kerhoas M. Lab Chip. 2015; 15:2388–2394. [PubMed: 25940789]
27. Lamparski HG, Metha-Damani A, Yao JY, Patel S, Hsu DH, Ruegg C, Le Pecq JB. J Immunol Methods. 2002; 270:211–226. [PubMed: 12379326]
28. Yamada T, Inoshima Y, Matsuda T, Ishiguro NJ. Vet Med Sci. 2012; 74:1523–1525.
29. Rider MA, Hurwitz SN, Meckes DG. Sci Rep. 2016; 6:23978. [PubMed: 27068479]
30. Wang Z, Wu H-j, Fine D, Schmulen J, Hu Y, Godin B, Zhang JXJ, Liu X. Lab Chip. 2013; 13:2879–2882. [PubMed: 23743667]
31. Li P, Kaslan M, Lee SH, Yao J, Gao Z. Theranostics. 2017; 7:789–804. [PubMed: 28255367]
32. Wu M, Ouyang Y, Wang Z, Zhang R, Huang PH, Chen C, Li H, Li P, Quinn D, Dao M, Suresh S, Sadovsky Y, Huang TJ. P Natl Acad Sci USA. 2017; 114:10584–10589.
33. Yang JS, Lee JC, Byeon SK, Rha KH, Moon MH. Anal Chem. 2017; 89:2488–2496. [PubMed: 28192938]
34. Ibsen SD, Wright J, Lewis JM, Kim S, Ko SY, Ong J, Manouchehri S, Vyas A, Akers J, Chen CC, Carter BS, Esener SC, Heller MJ. ACS Nano. 2017; 11:6641–6651. [PubMed: 28671449]
35. Lee K, Shao H, Weissleder R, Lee H. ACS Nano. 2015; 9:2321–2327. [PubMed: 25672598]
36. Cocucci E, Meldolesi J. Trends Cell Biol. 25:364–372.
37. Song X, Chen Y, Rong M, Xie Z, Zhao T, Wang Y, Chen X, Wolfbeis OS. Angew Chem Int Ed. 2016; 55:3936–3941.
38. Hu Y, Qian K, Yuan P, Wang Y, Yu C. Mater Lett. 2011; 65:21–23.
39. Ruth MC, Old WM, Emrick MA, Meyer-Arendt K, Aveline-Wolf LD, Pierce KG, Mendoza AM, Sevinsky JR, Hamady M, Knight RD, Resing KA, Ahn NG. J Proteome Res. 2006; 5:709–719. [PubMed: 16512687]
40. Lee H, Dellatore SM, Miller WM, Messersmith PB. Science. 2007; 318:426. [PubMed: 17947576]
41. Lee H, Rho J, Messersmith PB. Adv Mater. 2009; 21:431–434. [PubMed: 19802352]
42. Yan Y, Zheng Z, Deng C, Li Y, Zhang X, Yang P. Anal Chem. 2013; 85:8483–8487. [PubMed: 23941301]
43. Fang X, Zhao J, Zhang K, Yang P, Qiao L, Liu B. ACS Appl Mater Inter. 2016; 8:6363–6370.
44. Yan Y, Sun X, Deng C, Li Y, Zhang X. Anal Chem. 2014; 86:4327–4332. [PubMed: 24673251]
45. Skliar M, Chernyshev V, Belnap D, Hakami S, Stijleman I, Rachamadugu R, Bernard P. bioRxiv. 2017

46. Diaz G, Wolfe L, Kruh N, Dobos K. Sci Rep. 2016; 6:37975–37984. [PubMed: 27897233]
47. Fang X, Qiao L, Yan G, Yang P, Liu B. Anal Chem. 2015; 87:9360–9367. [PubMed: 26305297]
48. Gan J, Zhu J, Yan G, Liu Y, Yang P, Liu B. Anal Chem. 2012; 84:5809–5815. [PubMed: 22663254]
49. Trimpin S, Deinzer ML. Anal Chem. 2007; 79:71–78. [PubMed: 17194123]
50. Zhao Q, Liang Y, Yuan H, Sui Z, Wu Q, Liang Z, Zhang L, Zhang Y. Anal Chem. 2013; 85:8507–8512. [PubMed: 23957459]
51. Zhao Q, Fang F, Liang Y, Yuan H, Yang K, Wu Q, Liang Z, Zhang L, Zhang Y. Anal Chem. 2014; 86:7544–755. [PubMed: 24941313]
52. Wisniewski JR, Zougman A, Nagaraj N, Mann M. Nat Methods. 2009; 6:359–362. [PubMed: 19377485]
53. Kulak NA, Pichler G, Paron I, Nagaraj N, Mann M. Nat Methods. 2014; 11:319–324. [PubMed: 24487582]
54. Fan J, Shui W, Yang P, Wang X, Xu Y, Wang H, Chen X, Zhao D. Chem Eur J. 2005; 11:5391–5396. [PubMed: 16001450]
55. Blonder J, Goshe MB, Moore RJ, Pasa-Tolic L, Masselon CD, Lipton MS, Smith RD. J Proteome Res. 2002; 1:351–360. [PubMed: 12645891]
56. Mi H, Huang X, Muruganujan A, Tang H, Mills C, Kang D, Thomas PD. Nucleic Acids Res. 2017; 45:D183–D189. [PubMed: 27899595]
57. Ashburner M, Ball CA, Blake JA, Botstein D, Butler H, Cherry JM, Davis AP, Dolinski K, Dwight SS, Eppig JT, Harris MA, Hill DP, Issel-Tarver L, Kasarskis A, Lewis S, Matese JC, Richardson JE, Ringwald M, Rubin GM, Sherlock G. Nat Genet. 2000; 25:25–29. [PubMed: 10802651]

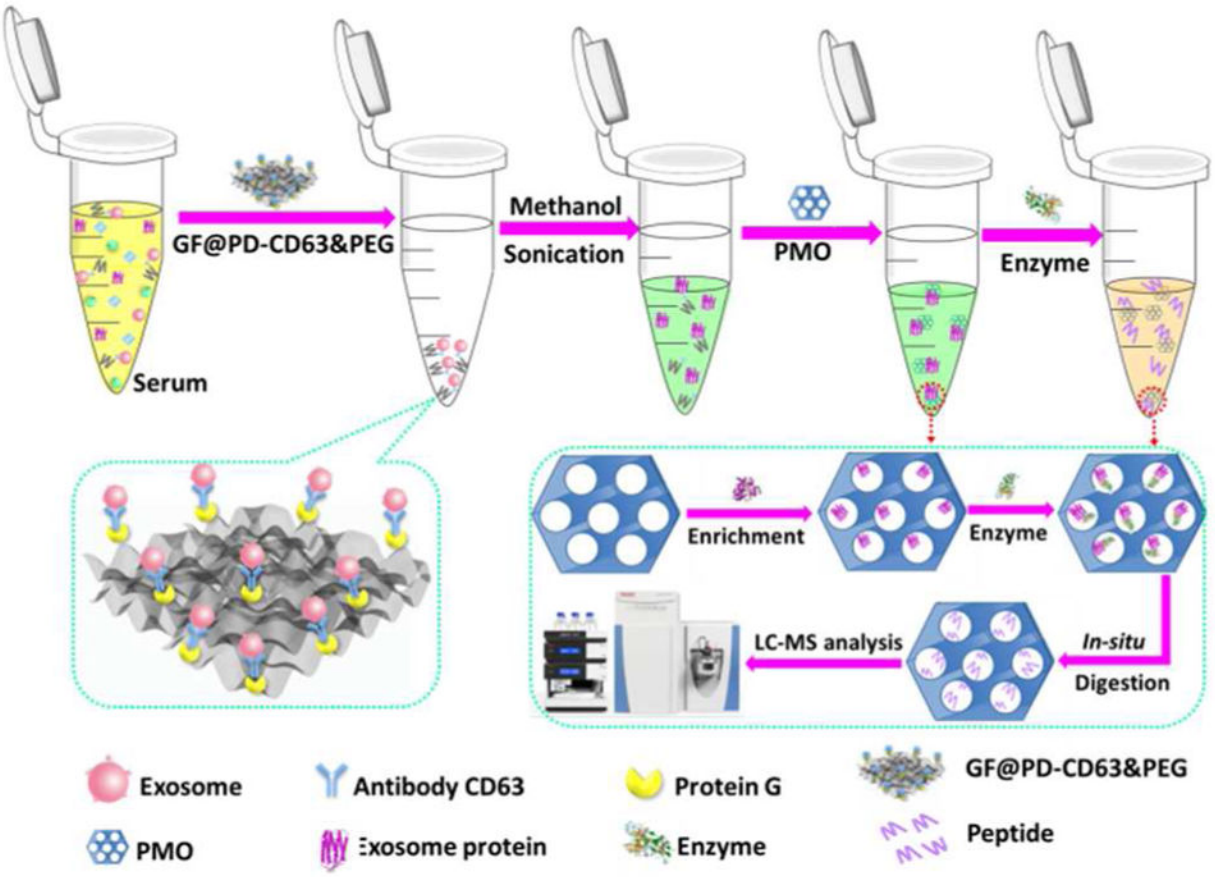

Figure 1.

Schematic Illustration of the Efficient Analysis Process for Exosomes Isolation and Protein Profiling by Using the Integrated Nanomaterial-based Platform.

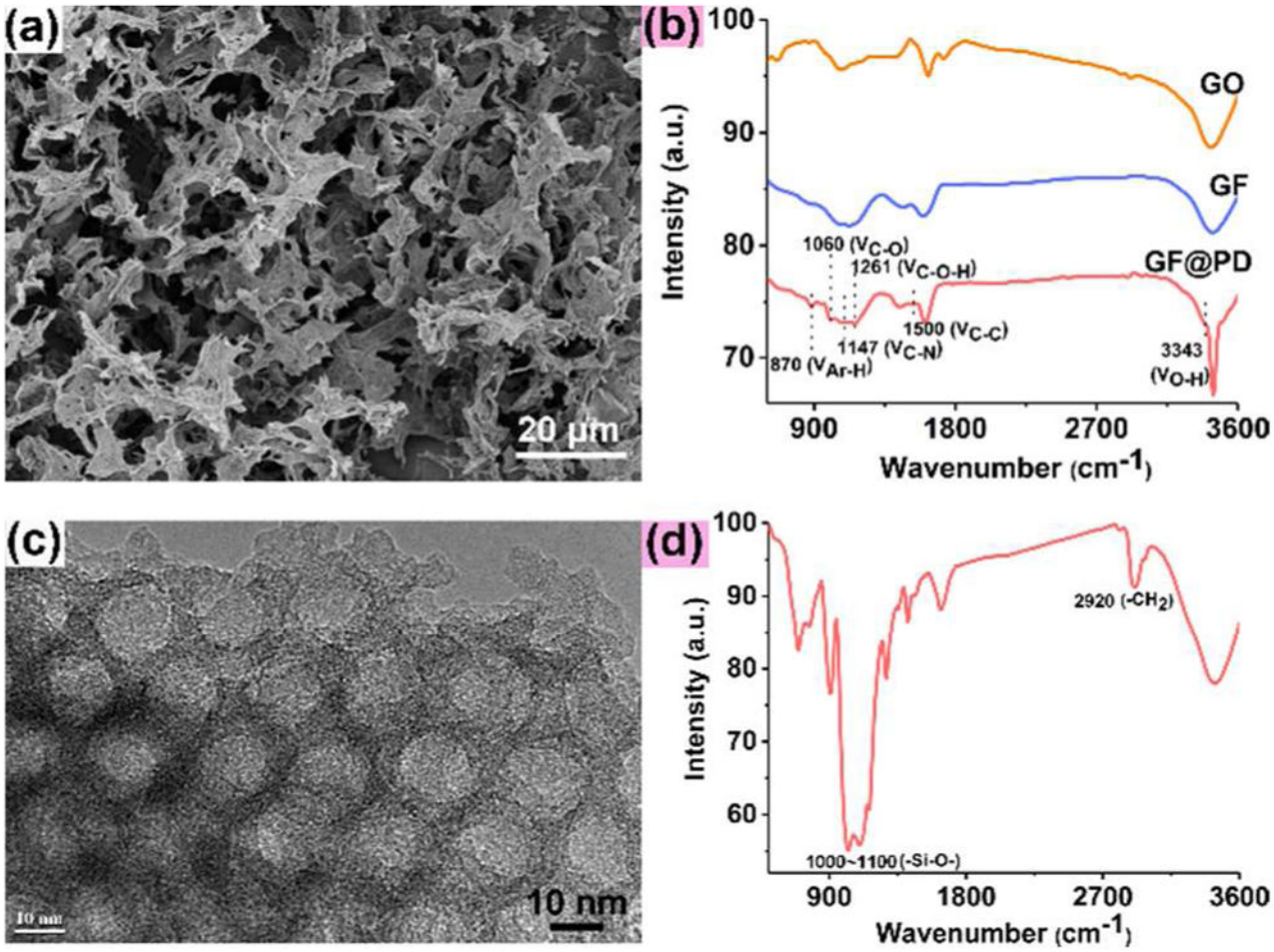

Figure 2.
a) SEM image and b) FT-IR of GF. c) SEM image and d) FT-IR of PMO.

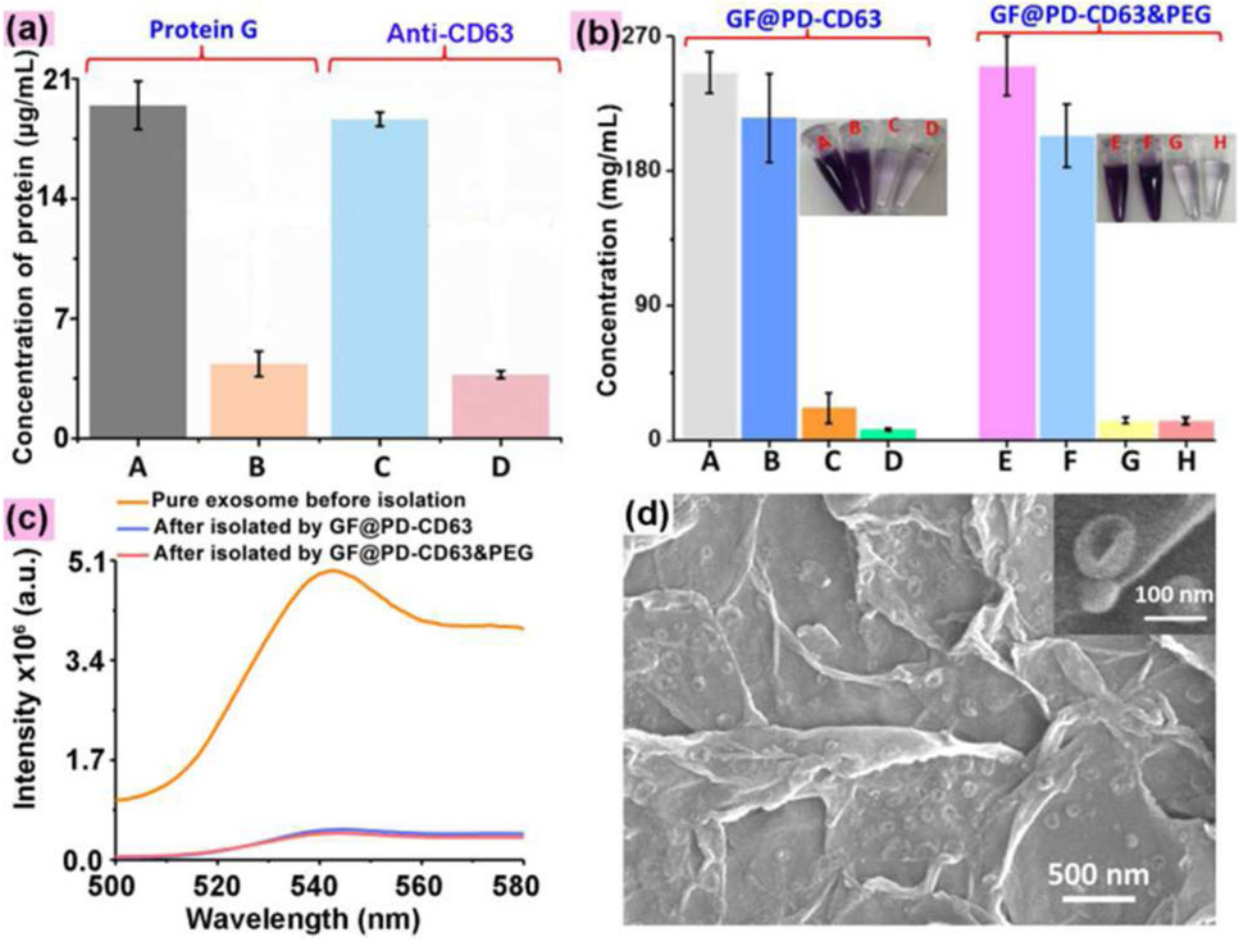

Figure 3.

a) Evaluation of protein G and CD63 immobilization on the surface of GF@PD. A and B represent the concentration of protein G in the solution before and after incubation with GF@PD. C and D are the concentration of CD63 in the solution before and after incubation with the protein G-modified GF@PD. b) Evaluation of protein binding to GF@PD-CD63 with or without PEG coating. A and B represent protein concentrations in serum before and after incubation with GF@PD-CD63, respectively. C shows the proteins eluted with 1× PBS buffer, and D indicated the proteins eluted after treatment with methanol. E, F, G, and H are equivalent to A, B, C, and D, respectively, but obtained with GF@PD-CD63&PEG. c) Fluorescence change of the DiO-stained exo-some sample before and after incubation with GF@PD-CD63 and GF@PD-CD63&PEG. d) SEM image of exosomes isolated by GF@PD-CD63&PEG. The error bars represented the standard deviation of three repeated measurements.

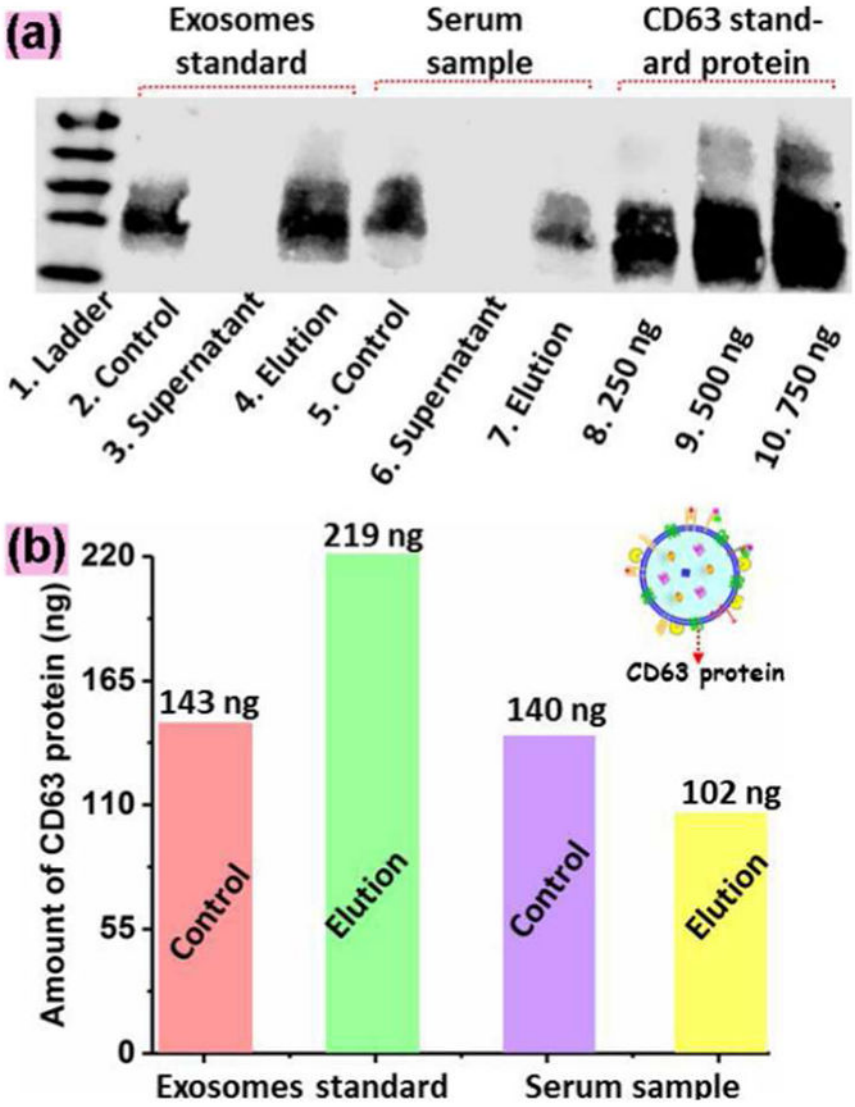

Figure 4.

a) Membrane image of and b) CD63 protein quantity found by Western Blot for analysis of CD63 recovered from the standard exosome solution and from human serum by GF@PD-CD63&PEG.

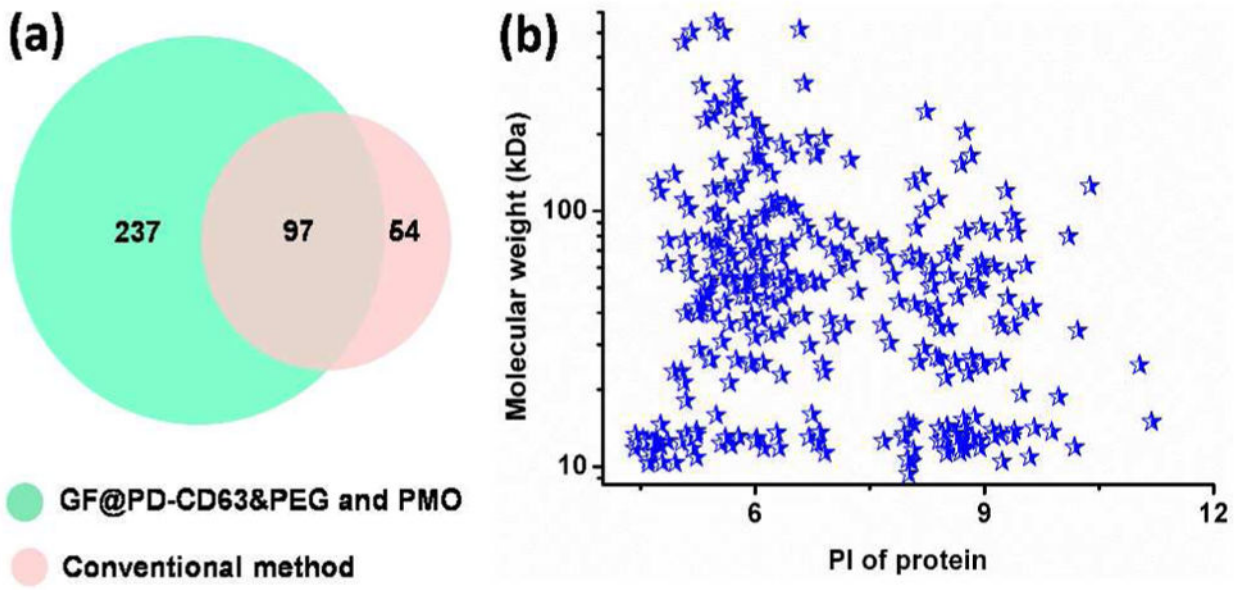

Figure 5.

(a) Venn diagram of the identified proteins by both the integrated GF/PMO platform and the conventional method. (b) Molecular weight and PI value distribution of the proteins identified by the integrated nanomaterial-based platform.

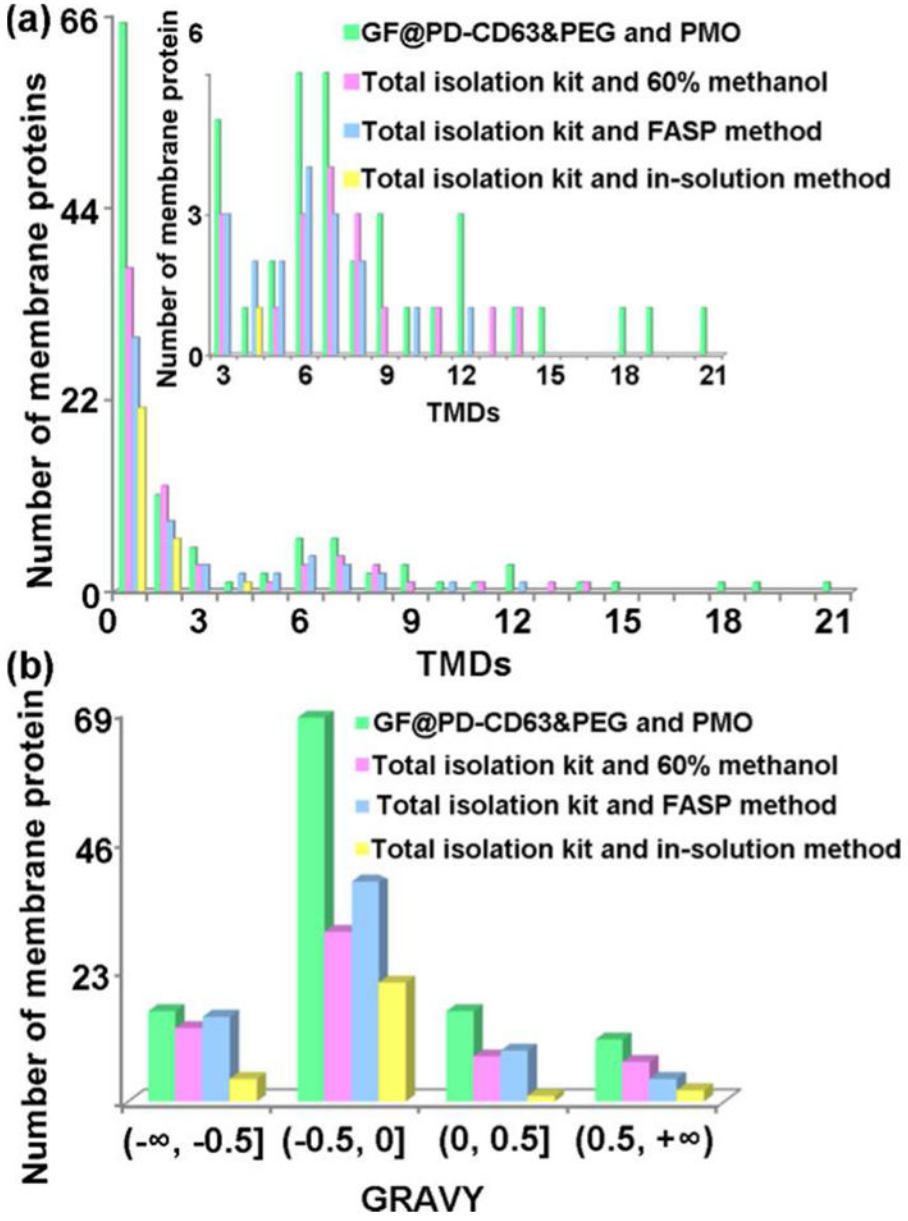

Figure 6.

Comparison of the distribution of (a) number of TMDs and (b) GRAVY values of the identified membrane proteins from serum exosomes by the integrated GF/PMO platform, 60% methanol, FASP, and in-solution digestion methods.